European Journal of Pharmaceutical Sciences 211 (2025) 107150

Contents lists available at ScienceDirect

European Journal of Pharmaceutical Sciences

journal homepage: www.elsevier.com/locate/ejps

Tiny-TIM intestinal fluids versus human intestinal fluids: A comparison of their composition and solubilizing capacity for poorly soluble drugs

Brecht Goovaerts [a], Álvaro López Mármol [b], Joachim Brouwers [a], Zahari Vinarov [c], Anura S. Indulkar [d], Thomas B. Borchardt [e], Patrick Augustijns [a,**], Mirko Koziolek [b,*]

[a] Drug Delivery and Disposition, KU Leuven, Herestraat 49, 3000 Leuven, Belgium
[b] NCE Drug Product Design and Development, AbbVie Deutschland GmbH & Co. KG, Ludwigshafen am Rhein, Germany
[c] Department of Chemical and Pharmaceutical Engineering, Sofia University, Dr. Marin Rousev Street No 4, 1164 Sofia, Bulgaria
[d] Development Sciences, Research and Development, AbbVie Inc., 1N. Waukegan Road, North Chicago, IL, 60064, United States
[e] Product Development Science & Technology, AbbVie Inc., 1N. Waukegan Road, North Chicago, IL, 60064, United States

ARTICLE INFO

Keywords:
Tiny-TIM
Food effect
Solubility
Intestinal fluid characterization
Lipids
Bile salts

ABSTRACT

The tiny-TIM system offers an *in vitro* platform for the simulation of physiological processes occurring in human stomach and small intestine aiding in drug product development by predicting the bioperformance of oral formulations under fasted and fed state intake conditions. To assess this *in vitro* system in terms of its physiological relevance, we performed a detailed analysis of the composition as well as the solubilizing capacity of tiny-TIM intestinal fluids (TIF), and compared this to previously collected and analysed human intestinal fluids (HIF). Moreover, the impact of meal type on TIF composition and solubilising capacity was investigated by using either a liquid meal or a solid meal. In the fasted state, TIF exhibited lower lipid concentrations with a TIF/HIF ratio of 0.27, and elevated bile salt levels (TIF/HIF ratio of 1.8). Fasted state TIF generally overpredicted the solubilizing capacity of HIF, likely due to its higher bile salt concentrations. In the fed state, TIF contained biorelevant lipid concentrations but remained monophasic without phase separation, unlike HIF. This was likely due to higher bile salt levels (5.3 times that of HIF), which solubilized all lipids into the micellar phase. This resulted on average in a 3.3-fold increase in solubility of the poorly water-soluble model compounds in the micellar fraction of TIF as compared to HIF. Shifting from a liquid to a solid meal had minimal impact on TIF composition and solubilizing capacity.

1. Introduction

In recent decades, the increasing prevalence of poorly water-soluble drug compounds has presented the pharmaceutical industry with the significant challenge of enabling adequate absorption following oral intake. Although various formulation strategies such as lipid-based formulations and amorphous solid dispersions have been developed to address this issue, accurately evaluating the bioperformance of these formulations during preclinical phases remains a challenge (Bennett-Lenane et al., 2020; Boyd et al., 2019). Among the tools available for such evaluations, the TNO gastrointestinal model (TIM) is recognized for its ability to closely replicate the physiology of the human gastrointestinal (GI) tract, providing a valuable *in vitro* platform for studying oral drug delivery and disposition (Butler et al., 2019; Vinarov et al., 2021).

Since its introduction by Minekus and colleagues over two decades ago, the TIM system has evolved from its initial applications in food sciences to becoming a valuable tool in supporting drug product development within the pharmaceutical industry (Minekus, 2015). The TIM-1 system simulates conditions in the upper gastrointestinal tract and consists of four separate chambers representing the stomach, duodenum, jejunum, and ileum. Within these compartments, processes such as peristalsis, secretion, transfer of luminal contents, digestion, and filtration are simulated in a controlled manner (Minekus, 2015). More recently, the introduction of the tiny-TIM, a fully automated, commercially available bench-top version which only includes the gastric compartment and a single intestinal compartment, has provided the pharmaceutical industry with a more accessible tool for drug product

* Corresponding author at: Drug Product Design and Development, AbbVie Deutschland GmbH & Co. KG, Ludwigshafen am Rhein, Germany.
** Corresponding author at: Drug Delivery and Disposition, Gasthuisberg O&N 2, Herestraat 49, box 921, KU Leuven, 3000 Leuven, Belgium.
E-mail addresses: patrick.augustijns@kuleuven.be (P. Augustijns), mirko.koziolek@abbvie.com (M. Koziolek).

https://doi.org/10.1016/j.ejps.2025.107150
Received 10 March 2025; Received in revised form 5 May 2025; Accepted 28 May 2025
Available online 10 June 2025

development (Schilderink et al., 2020). Despite its high biorelevance, tiny-TIM is mainly used in the later stages of the preclinical phase and in the clinical phase because of relatively low throughput and high costs. However, it has been successfully applied for different purposes, such as formulation ranking, dosage optimization, and food effect prediction (Chiang et al., 2022; Liu et al., 2024; López Mármol et al., 2022; Schilderink et al., 2020; Verwei et al., 2016). The latter is of particular interest, as the design of the system allows for the realistic simulation of digestive processes under both fasted and fed state conditions, thereby offering insights into the potential impact of food on *in vitro* drug release.

In its effort to evaluate the behaviour of drug products in a highly biorelevant manner, the tiny-TIM dynamically generates simulated intestinal fluids (SIF) based on the initial contents of the gastric compartment, its secretions, and its transit conditions. The composition of the fluids may play a critical role in, for instance, the solubilization of poorly water-soluble drug compounds. However, to the best of our knowledge, a comprehensive assessment of the biorelevance of these SIF, hereafter referred to as tiny-TIM intestinal fluids (TIF), has not yet been conducted. This underscores the necessity of a detailed evaluation of the fluids produced by the tiny-TIM system, particularly in comparison to human intestinal fluids (HIF). A previous study by Pentafragka et al. performed such a comparison using the TIM-1 system, but was limited by differences between *in vitro* and *in vivo* setups, and by a narrow focus on compositional parameters such as bile salt concentrations and pH (Pentafragka et al., 2022). Additionally, their study assessed the dissolution, rather than equilibrium solubility, of only two model compounds.

The present study was undertaken to address the need for a more precise evaluation of the biorelevance of the tiny-TIM system, by means of a direct analysis of the composition as well as the solubilizing capacity of TIF, while making a comparison to previously collected and analysed HIF from the upper small intestine. Furthermore, this study investigated the impact of meal type, *i.e.*, a liquid meal or a solid meal, on the composition of TIF and its solubilizing capacity for seven poorly water-soluble model compounds.

2. Materials and methods

2.1. Materials

For the TIF collection, acetic acid 96 %, calcium chloride dihydrate, disodium hydrogen phosphate, hydrochloric acid 1 M, potassium chloride, sodium chloride, sodium hydrogen carbonate, sodium dihydrogen phosphate monohydrate and sodium hydroxide solution 1 M were purchased from Merck KGaA (Darmstadt, Germany). Sodium acetate-trihydrate and sodium hydroxide (pellets) were purchased from Honeywell International Inc. (Seelze, Germany). Potassium chloride was purchased from Fluka Analytical (München, Germany). Hydroxypropyl methyl cellulose (HPMC) was purchased from Colorcon GmbH (Idstein, Germany). α-Amylase from *Bacillus sp*.-Type II-A, lipase from *Rhizopus oryzae*, pancreatin from porcine pancreas (8X USP specifications), pepsin from porcine gastric mucosa, porcine bile extract, sodium chloride, sodium citrate tribasic dihydrate and trypsin from porcine pancreas were purchased from Sigma-Aldrich Chemie GmbH (Schnelldorf, Germany). Porcine bile was purchased from InnoGI Technologies (Zeist, Netherlands). Plasma filters (Plasmaflux P1 dry) were purchased from Fresenius Medical Care (Bad Homburg, Germany). For filter rinse and recovery of itraconazole, ethanol 70 % was purchased from VWR International GmbH (Darmstadt, Germany).

For the characterization of the tiny-TIM fluids and solubility experiments, taurochenodeoxycholic acid (TCDC), taurodeoxycholic acid (TDC), glycoursodeoxycholic acid (GUDC), glycochenodeoxycholic acid (GCDC), glycodeoxycholic acid (GDC), glycocholic acid (GC), chenodeoxycholic acid (CDC), deoxycholic acid (DC), lithocholic acid (LC), cholic acid (C), sodium hydroxide (NaOH), cholesterol (Chol), cholesteryl oleate, cholesteryl palmitate (Cholp), tripalmitin (TP), triolein, trilinolein, dipalmitin, diolein, dilinolein (DL), mono-oleate (MO), mono-palmitin, mono-linolein, palmitic acid, oleic acid (OA), linoleic acid, 1-octadecanol, L-tryptophan, ritonavir, danazol, nifedipine and orlistat were purchased from Sigma-Aldrich (St. Louis, MO). Tauroursodeoxycholic acid (TUDC), ursodeoxycholic acid (UDC), and taurocholic acid (TC) were acquired from Calbiochem (Darmstadt, Germany). Taurohyocholic acid (THC), glycohyocholic acid (GHC) and glycohyodeoxycholic acid (GHDC) were purchased from Sanbio B.V. (Uden, The Netherlands). Taurohyodeoxycholic acid (THDC) was acquired from Tebu-bio (Heerhugowaard, The Netherlands). Deuterated cholic acid (d4) was purchased from Cayman Chemical (Ann Arbor, MI). The internal standards for itraconazole (D5) and chenodeoxycholic acid (d4) were bought from Alsachim (Illkirch Graffenstaden, France). Hydrochloric acid (HCl) and acetonitrile (ACN, HPLC gradient grade) were purchased from Fischer Scientific (Waltham MA) and methanol (MeOH, HPLC grade) from Acros Organics (Waltham MA). MeOH and formic acid (FA) LC/MS grade were acquired from Biosolve (Valkenswaard, The Netherlands). Isooctane (UV spec grade), ethyl acetate (LC-MS grade) and acetone (LC-MS grade) were purchased from Carl Roth (Karlsruhe, Germany). Acetic acid was bought from Chem-Lab Analytical (Zedelgem, Belgium). Cabozantinib was purchased from Bionet Key Organics (Cornwall, UK). Itraconazole and etravirine were kindly provided by Janssen Pharmaceutica (Beerse, Belgium). Posaconazole was bought from Biosynth Ltd. (Compton, UK). Ensure Plus was purchased from Abbott Laboratories B.V. (Zwolle, The Netherlands). Purified water was produced using a Purelab® Flex water system from Veolia (Paris, France). All substances used for solubility experiments had a purity above 95 %.

2.2. Media collection

2.2.1. Human intestinal fluid

The collection of HIF and its characterization in terms of composition and solubilising capacity was described previously in a study by Goovaerts et al. (Goovaerts et al., 2024). In brief, during a study at UZ Leuven, approved by the Ethics Committee Research UZ/KU Leuven (S53791), intestinal fluids from 21 healthy volunteers (9 women and 12 men, aged 21–56, BMI 18–26 kg/m^2) were collected (see Fig. 2). Volunteers fasted for 12 h before a catheter was placed in their duodenum (D2-D3) for fluid collection. After drinking 240 mL of water, fasted state samples were taken every 10 min for 90 min. Subsequently, 400 mL of Ensure Plus was administered to simulate fed state conditions. After 20 min, 240 mL of water was consumed, marking the start of the fed state fluid sampling, conducted identical to the fasted state sampling. Fluids were treated with orlistat (final concentration of 1 μM) to prevent post-sampling lipolysis and stored at −26 °C. Samples were pooled into fasted, early fed, and late fed states for analysis, resulting in 21 pools (7 of each state) consisting of 3 randomly assigned volunteers per group.

2.2.2. Tiny-TIM intestinal fluid

TIF were collected from the intestinal compartment of the tiny-TIM system in the fasted, early fed and late fed states for direct comparison with HIF fluids. Blank tiny-TIM runs were initiated in both the fasted and fed state, and subsequently interrupted to empty the intestinal compartment and to collect all intestinal fluid. Depending on the prandial state, the runs were interrupted after 45 min (fasted and early fed state) or 90 min (late fed state). In the fed state, two distinct meals were used, a liquid meal and a solid meal.

2.2.2.1. The tiny-TIM. The tiny-TIM system (InnoGI Technologies, Zeist, Netherlands) is a dynamic, computer-controlled, two-compartmental *in vitro* model of the stomach and the upper small intestine (Fig. 1) (Minekus, 2015). A comprehensive description of the system's design and functionality has been provided by López Mármol et al. (López Mármol et al., 2022), to which we refer readers for further

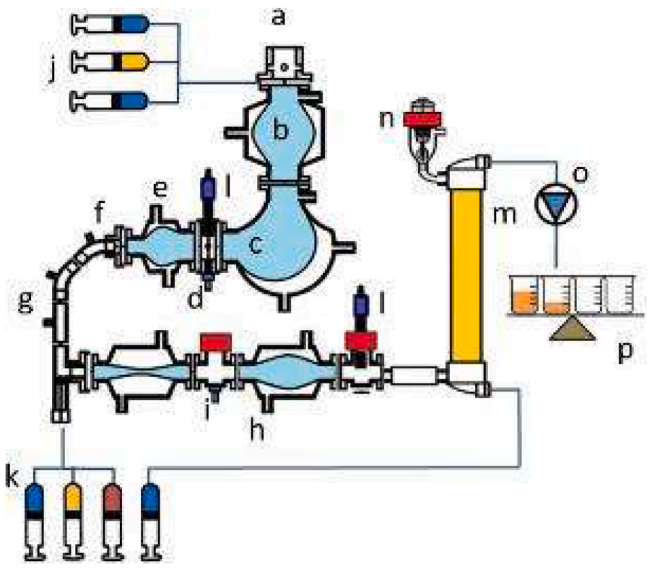

Fig. 1. Graphical representation of the tiny-TIM model including an advanced gastric compartment (AGC). a: meal inlet, b: corpus, c: proximal antrum, d: gastric port, e: distal antrum, f: pyloric valve, g: peristaltic valve, h: small intestinal compartment, i: small intestinal port, j: gastric secretions, k: intestinal secretions, l: pH electrodes, m: filtration system, n: level sensor, o: sample pump, p: sample bottles. The pyloric and peristaltic valves (f, g) mimic the function of the pylorus and successively open and close enabling the emptying of the gastric chyme into the small intestinal compartment. The single intestinal compartment (h) simulates the transit of the chyme through the upper small intestine. All fluids entering the small intestinal compartment are removed through a filtration system (m) and collected in sample bottles (p) at predefined time intervals. Adapted with permission from López Mármol et al. "Application of tiny-TIM as a mechanistic tool to investigate the *in vitro* performance of different itraconazole formulations under physiologically relevant conditions" (López Mármol et al., 2022). Copyright 2022 Eur J Pharm Sci.

details.

To enable the evaluation of multiple protocols in this work, it was decided to test all experimental conditions as single measurements ($n = 1$). Key control parameters including the simulated pH profiles and the rates of fluid secretion were individually evaluated for each single run to ensure a proper functioning of the system within the acceptance limits. In addition, previously published studies provided evidence of the low variability between tiny-TIM runs (Pentafragka et al., 2022; Verwei et al., 2016).

2.2.2.2. Solution and reagents preparation. Several solutions and reagents were prepared for the tiny-TIM experiments to simulate fasted and fed states, including gastric and small intestinal electrolyte solutions (GES and SIES), HPMC and bile solutions for simulating gastric viscosity and bile reflux from the duodenum to the stomach, and enzyme solutions containing lipase, pepsin and amylase. Preparation procedures have been described in a study by López Mármol et al. (López Mármol et al., 2022). Gastric start residue was added to the meal shortly before the start of the experiment and is composed of 1800 U amylase (only in the fed state), HPMC 0.4 % and bile 0.04 % solution.

2.2.2.3. Experimental conditions. Initially, the stomach compartment was filled with buffered solution in fasted state experiments or the corresponding meal in fed state experiments. After the pre-adjustment of the gastric compartment pressure to 80 ± 5 mbar, the run was initiated. For fed state runs, the standard experimental protocol for fed studies considering the intake of a high-fat meal (t1/2: 80 min, gastric residence time: 180 min), was used.

The experimental conditions of the fasted and fed state protocols are summarized in Table 1.

Table 1
Experimental settings in tiny-TIM protocols for the simulation of fasted and fed state conditions.

Parameter	Fasted	Fed state (liquid meal)	Fed state (solid meal)
Gastric medium composition	213 g water, 27 g citrate buffer (1 M), 30 g gastric start residue	200 mL Ensure Plus, 70 g GES (1x), 70 g water, 10 g gastric start residue	150 g high-fat meal, 70 g GES (1x), 70 g water, 10 g gastric start residue
Initial gastric medium pH	pH 3.0	pH 6.5	pH 6.5
Initial gastric content (g)	270 *g*	300 *g*	300 *g*
Gastric pH	Stepwise reduction from pH 3 to pH 1.7 within 60 min	Not controlled (HCl secretion based on natural flow curve of the reacidifying stomach)	Not controlled (HCl secretion based on natural flow curve of the reacidifying stomach)
Concentration of administered gastric acid	1 M	0.3 M	0.3 M
Small intestinal pH	pH 6.7 ± 0.3	pH 6.7 ± 0.3	pH 6.7 ± 0.3
Porcine bile concentration (v/v)	20 %	Undiluted (100 %)	Undiluted (100 %)

In the fed state, either a liquid or a solid meal was administered, with their volumes adjusted to accommodate the 300 mL capacity of the advanced gastric compartment. For the liquid meal, Ensure Plus was used to ensure uniformity with the meal used to collect HIF. For the solid meal, a homogenised (Solostar® 4 Horizontal Slow Masticating Juicer, Tribest, Anaheim *CA*, USA) high-fat meal as recommended by the FDA was used, which was composed of eggs, butter, bacon, rusk, potatoes, full-fat milk, margarine and tap water (FDA, 2002). This meal was prepared in a larger batch (2320 g) and aliquots were stored for maximum 6 months at −18 °C until usage. For each TIM run in which the intake of a high-fat meal was simulated, an aliquot of 150 g with a total caloric value of 238 kcal (caloric composition: 55 % from fat, 15 % from proteins, 30 % from carbohydrates) was used. In comparison, 200 mL of Ensure Plus contains 300 kcal (caloric composition: 29 % from fat, 17 % from proteins, 54 % from carbohydrates).

The gastric and intestinal pH profiles, gastric emptying kinetics, and details about the filter used in the TIM-runs were identical to those reported in a study by López Mármol *et al.* (López Mármol et al., 2022). A standard filtration rate of 3.9 mL/min was applied.

2.2.2.4. TIF collection. To collect the intestinal contents, the TIM-run was interrupted at 45 min after initiation (fasted and early fed state) or at 90 min (late fed state). The contents were collected via the small intestinal port (Fig. 1) and lipolysis was immediately inhibited by using 0.5 µL/mL of a 500 mM stock solution of the lipase inhibitor 4-bromophenylboronic (4-BBA) acid in DMSO. This resulted in a final concentration of 2.5 mM 4-BBA and a minor but negligible addition of DMSO to the samples (0.05 %, v/v). Samples were aliquoted to limit freeze-thaw cycles and subsequently stored at −26 °C.

In Fig. 2, the protocols for collection of HIF and TIF are summarized in a schematic manner.

2.3. Characterisation of intestinal fluids

The TIF and HIF pools were characterized for total lipids (triglycerides [TAGs], diacylglycerides [DAGs], monoacylglycerides [MAGs], and free fatty acids [FFAs]), bile salts, phospholipids, total cholesterol (cholesterol and cholesteryl esters), pH and total protein. Characterization was performed on (i) the micellar (aqueous) fraction, and (ii) the total sample consisting of both the micellar fraction and the

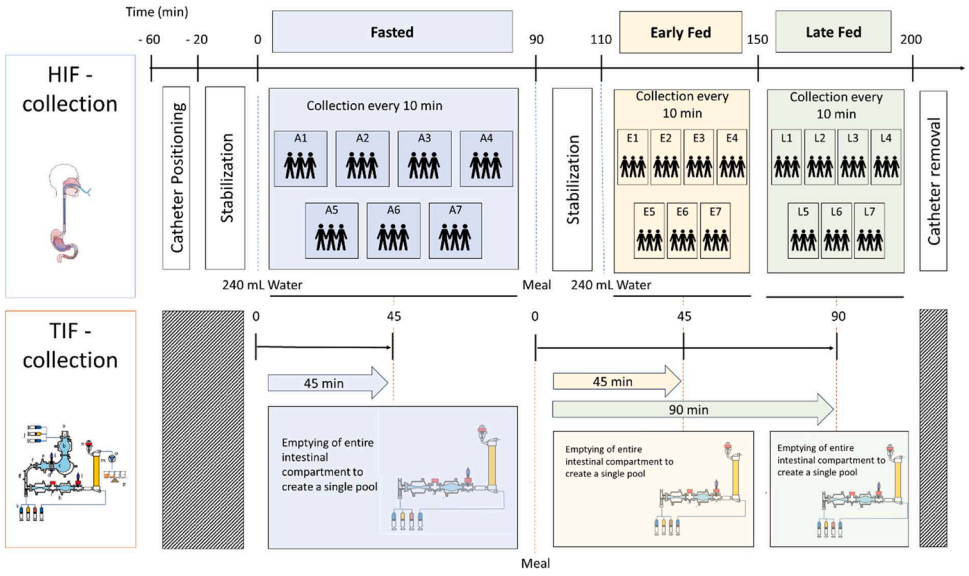

Fig. 2. Graphical representation of intestinal media collection from both humans and the tiny-TIM in fasted, early fed and late fed states. A: fasted state, E: early fed state, L: late fed state. Tiny-TIM graphical representation adapted with permission from López Mármol *et al.* "Application of tiny-TIM as a mechanistic tool to investigate the *in vitro* performance of different itraconazole formulations under physiologically relevant conditions" (López Mármol et al., 2022). Copyright 2022 Eur J Pharm Sci. Image on HIF-collection adapted with permission from Goovaerts *et al.* "Understanding the Impact of Lipids on the Solubilizing Capacity of Human Intestinal Fluids" (Goovaerts et al., 2024). Copyright 2024 American Chemical Society.

lipid fraction. The total sample was taken as such, while the micellar sample was isolated by centrifugation (30 min, 20 000 g, 37 °C) (Centrifuge 5804 R, VWR International, Leuven, Belgium) and subsequent removal of the upper lipid fraction using a glass pipette connected to a vacuum pump. The centrifugation and lipid removal were repeated a second time to account for unwanted mixing during the first lipid removal step. The resulting aqueous colloidal fraction was consistently transparent prior to analysis. Therefore, this fraction is referred to as the "micellar fraction", as it consisted predominantly of micelles.

2.3.1. *pH*

The pH value was determined using a BioTrode glass electrode (Hamilton, Reno, NV, USA), which was calibrated before each use.

2.3.2. *Total protein*

Total protein concentration was determined using the tryptophan fluorescence assay described by Wisniewski *et al.* (Wiśniewski and Gaugaz, 2015). In short, 2 µL of intestinal fluid was added to 200 µL 8 M urea in 100 mM tris-aminomethane pH 7.8. Fluorescence (excitation 295 nm, emission 350 nm) was measured using a Tecan infinite m200 plate reader (Tecan, Männedorf, Switzerland), and compared to a calibration curve of different tryptophan concentrations. Total protein content was calculated assuming an average tryptophan content of 1.17 %.

2.3.3. *Bile salts*

Bile salts were quantitatively measured with LC-MS/MS using a Xevo TQ-S (Waters Milford, MA, USA), according to the method described by Goovaerts *et al.* (Goovaerts et al., 2024). The method was further optimised to the use of porcine bile in TIF by adding four additional quantifiable bile salts: glycohyodeoxycholic acid (GHDC), glycohyocholic acid (GHC), taurohyodeoxycholic acid (THDC) and taurohyocholic acid (THC).

2.3.4. *Phospholipids*

The concentration of phospholipids was determined using the LabAssay™ Phospholipid kit (Fujifilm, Tokyo, Japan). Phospholipids containing choline were hydrolyzed to choline by phospholipase D. Choline was subsequently oxidized by choline oxidase producing hydrogen peroxide which in turn reacted with N-ethyl-N-(2-hydroxy-3-sulfopropyl)-3,5-dimethoxyaniline (DAOS) and 4-aminoantipyrine resulting in a blue colour. The phospholipid concentration was then determined by measuring the absorbance (600 nm) using a Tecan infinite m200 plate reader (Tecan, Männedorf, Switzerland).

2.3.5. *Lipids and cholesterol*

Total lipids were determined with high-performance liquid chromatography (HPLC) coupled to a charged aerosol detector (CAD) (Thermo Fisher Scientific, Waltham, MA) using a method adapted from Infantes-Garcia *et al.* (Infantes-Garcia et al., 2021). For a detailed explanation of the analytical method, we refer to Goovaerts et al. (Goovaerts et al., 2024).

2.4. *Apparent solubility of selected model compounds*

2.4.1. *Solubility assay*

The equilibrium solubility of seven poorly water-soluble model compounds (*i.e.,* ritonavir, nifedipine, cabozantinib, etravirine, itraconazole, danazol and posaconazole) was determined in the TIF pools, and subsequently compared to solubility data in HIF, which were previously assessed using the same procedure (Goovaerts et al., 2024). Compounds were selected based on their poor water solubility, lipophilicity and diverse food effect outcomes. The most important physicochemical properties are included in Table 2. The selected compounds are predominantly unionised at intestinal pH, in order to mitigate the effect of pH on the intrinsic aqueous solubility of the compounds and increase the sensitivity to solubilisation. All solubility values reported in this manuscript should be considered apparent, *i.e.*, including both molecules freely dissolved in the aqueous phase and molecules solubilized in colloidal structures and lipid droplets (Vertzoni et al., 2022).

In fed state fluids, solubility was determined in the micellar fraction and in the total sample (micellar and lipid fractions combined). In fasted state fluids, solubility was determined in the total sample only, as these fluids did not contain a lipid fraction. All solubility values were determined in triplicate. In fed state fluids, bacterial degradation was prevented by the addition of a penicillin/streptomycin mixture in water

Table 2
Physicochemical properties of the seven model compounds. Table adapted with permission from Goovaerts et al. "Understanding the Impact of Lipids on the Solubilizing Capacity of Human Intestinal Fluids". Copyright 2024 American Chemical Society (Goovaerts et al., 2024).

Compound	Molecular weight (g/mol)	Acid/base/non-ionizable	pK_a*	LogP
Ritonavir	720.9	base	4.46, 2.47	5.6 (Yu et al., 2020)
Nifedipine	346.3	base	1.28	2.50 (van der Lee et al., 2001)
Cabozantinib	501.5	base	5.3	5.3 (Williams et al., 2018)
Etravirine	435.3	base	2.77	> 5 (Schöller-Gyüre et al., 2009)
Itraconazole	705.6	base	3.7	6.2 (Bhardwaj et al., 2013)
Danazol	337.5	non-ionizable	/	4.53 (Kumar et al., 2015)
Posaconazole	700.8	base	3.6, 4.6	5.41 (Steuer et al., 2016)

* pK_a values were generated using ADMET predictor.

(both 10 000 U/mL) using a 1/100 dilution ratio (final activity: 100 U/mL).

To an excess of crystalline drug powder (1 mg for all compounds, with the exception of 0.6 mg for cabozantinib), 300 μL of TIF was added. Subsequently, the suspension was incubated at 37 °C for 24 h under continuous shaking at 175 RPM (IKA KS 4000i control, Staufen, Germany) to reach equilibrium solubility, followed by centrifugation (30 min, 20 000 g, 37 °C). The 24-hour incubation period was selected based on prior time-dependent solubility studies confirming equilibrium solubility for all compounds within this timeframe.

2.4.2. Sample preparation

After centrifugation of TIF, multiple fractions were obtained: the undissolved solid material at the bottom, the aqueous micellar fraction, and the lipid fraction on top, the latter being present in the majority of fed state samples. The micellar fraction was isolated by removing the upper lipid fraction using a glass pipette connected to a vacuum pump. The centrifugation (30 min, 20 000 g, 37 °C) and lipid removal using suction were repeated a second time to account for unwanted mixing during the first suction step. Using separate aliquots, the isolation of the total sample (micellar and lipid fractions combined) required the transfer of both lipid and micellar fractions to a new vial, thus leaving the undissolved solid material behind. The micellar and lipid fractions were subsequently re-homogenized to obtain the total sample, using a vortex. Before quantification, samples were either diluted in 50:50 MeOH/H_2O or with ice cold MeOH + 1 % FA for protein precipitation, followed by a centrifugation step (10 min, 20 000 g, 4 °C). As itraconazole was analysed using MS detection, an internal standard (H^5-itraconazole) was added to (50:50) MeOH/H_2O at a final concentration of 50 nM.

2.4.3. LC analysis

The diluted samples were analysed using (U)HPLC with UV absorbance, fluorescence or tandem MS detection, depending on the compound (Table 3). Detailed information about the analytical setup used for the model compounds has been described by Goovaerts et al. (Goovaerts et al., 2024).

3. Results

In this study, tiny-TIM intestinal fluids (TIF) were collected under both fasted and fed state conditions and compared to earlier collected human intestinal fluids (HIF). For the fed state, two different meal types were administered to the tiny-TIM in separate runs: a liquid and a solid meal. The collected fluids were thoroughly characterized and subsequently used in solubility studies for seven model compounds.

Table 3
Sample preparation and separation of model compounds. Table adapted with permission from Goovaerts et al. "Understanding the Impact of Lipids on the Solubilizing Capacity of Human Intestinal Fluids" (Goovaerts et al., 2024). Copyright 2024 American Chemical Society.

Compound	Sample Dilution	Mobile Phase	Injection volume	Flow rate	Detection
Ritonavir	MeOH: H_2O (1:20 v/v)	MeOH: Buffer[1] (80:20)	50 μL	1 mL/min	UV: 241 nm
Nifedipine	MeOH:H_2O (1:100 v/v)	ACN: Buffer[1] (60:40)	50 μL	1 mL/min	UV: 340 nm
Cabozantinib	MeOH: H_2O (1:100 v/v)	MeOH: Buffer[2] (72:28)	50 μL	1 mL/min	UV: 322 nm
Etravirine	MeOH:H_2O (1:100 v/v)	MeOH: Buffer[1] (80:20)	50 μL	1 mL/min	UV: 312 nm
Itraconazole	MeOH:H_2O 1:25 v/v (Fasted) 1:250 v/v (Fed)	MeOH: H_2O w/ 0.05 % FA	2 μL	0.6 mL/min	MS/MS
Danazol	MeOH:H_2O (1:100 v/v)	MeOH: H_2O (82:18)	50 μL	1 mL/min	UV: 285 nm
Posaconazole	MeOH 1 % FA (1:10 v/v)	MeOH: Buffer[1] (82:18)	50 μL	1 mL/min	Fluo: *ex* 240 nm *em* 385 nm

Buffer[1]: 25 mM Acetic acid in H_2O at pH 3.5.
Buffer[2]: 40 mM formic acid in H_2O at pH 2.5.

The study focused on comparing the composition and solubilizing capacity of the fluids in two different ways: (I) between HIF and TIF, after the ingestion of a liquid meal and (II) between TIF obtained after the ingestion of either a liquid meal or a solid meal. In all experiments, a distinction was made between micellar samples and total samples (*i.e.*, lipid and micellar fraction combined).

3.1. Comparison between TIF and HIF

This section compares the composition and solubilising capacity of TIF and HIF. To ensure optimal comparison, the TIM runs were collected upon pausing the run at the midpoint of the collection period of the HIF samples (*i.e.* after 45 min in both the fasted and early fed state, and after 90 min in the late fed state) (see Fig. 2). This comparison is limited to fasted state tiny-TIM runs and runs following the ingestion of a liquid meal, as the same meal was used in the HIF aspiration studies.

3.1.1. Composition

A comprehensive characterization of the fasted, early fed, and late fed state TIF was conducted and compared to the composition of HIF. This analysis focused on the concentrations of total lipids (TAGs, DAGs, MAGs and FFAs), bile salts, phospholipids, total cholesterol (cholesterol and cholesteryl esters), pH, and total protein. For the fed state fluids, all factors except for pH were quantified in both the micellar sample and the total sample. Results are summarised in Fig. 3.

3.1.1.1. Lipids and lipid digestion products. Fig. 3 illustrates the cumulative concentrations of TAG and its digestion products (DAG, MAG, and FFA), collectively referred to as 'total lipids.' In the fasted state, TIF contained relatively low lipid concentrations, with 0.17 mg/mL at 45 min after the start of the run. This concentration is considerably lower compared to the fasted state HIF, which averaged at 0.63 mg/mL, yielding a TIF/HIF ratio of 0.27.

In the early fed state, the lipid concentration in the total samples of

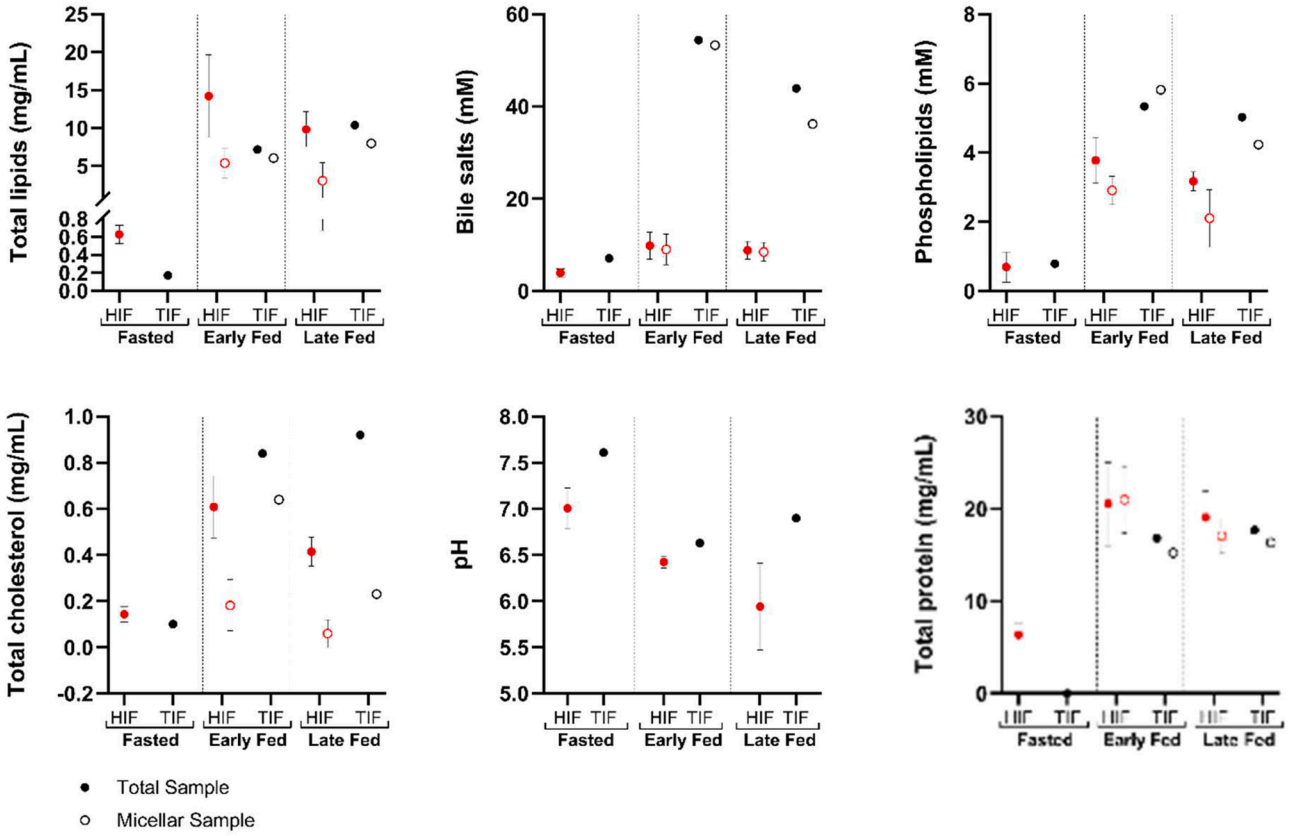

Fig. 3. Composition of HIF (red dots) and TIF (black dots) with respect to lipids (*i.e.*, TAGs, DAGs, MAGs and FFAs), bile salts, phospholipids, total cholesterol (*i.e.*, cholesterol and cholesteryl esters), pH, and total protein. Characterization was divided into a fasted state, an early fed state and a late fed state. In the fed state, the total (closed dots) and micellar samples (open dots) were separated for all compositional characteristics except for pH. Data points represent the mean ± SD of seven distinct HIF pools, and a single TIF pool.

TIF was approximately half of the average concentration found in HIF, with concentrations of 7.14 mg/mL and 14.2 mg/mL, respectively. However, by the late fed state, similar lipid concentrations were observed in the total samples of TIF (10.37 mg/mL) and HIF (9.8 mg/mL).

Apparent differences were observed when comparing total sample lipid concentrations to micellar lipid concentrations. In fed state HIF (early and late fed state combined), the removal of the lipid fraction resulted in an average threefold decrease in lipid concentration, dropping from 12 mg/mL to 4.1 mg/mL (66 % reduction). In contrast, fed state TIF showed only a minor reduction in lipid concentration after centrifugation and the removal of the upper fraction, decreasing from 8.8 mg/mL to 7.0 mg/mL (20 % reduction).

Visual comparison of the fluids, as shown in Fig. 4, revealed that fed state TIF, unlike fed state HIF, did not visibly contain a separate lipid fraction. HIF was a multi-phase fluid that could be separated into distinct fractions after centrifugation: a lipid fraction, a micellar fraction, and a solid pellet. TIF, however, could only be separated into a micellar fraction and a solid pellet, indicating the minimal presence of a distinct lipid fraction.

In addition to differences in total lipid concentration, there were notable differences in lipid composition between HIF and TIF in both fasted and fed state. As shown in Fig. 5, HIF predominantly contained FFAs, accounting for an average of 91.9 % (m/m) of the lipid content, with minimal amounts of TAG, DAG, and MAG, indicating almost complete lipolysis. In contrast, while TIF also exhibited complete digestion of TAG and DAG, MAG remained largely undigested. This resulted in a composition of approximately 65.1 % (m/m) FFA and 32.9 % (m/m) MAG in TIF. The lipid composition in TIF was consistent across the fasted, early and late fed pools (n = 3), with relative standard deviations (RSD) of 7.2 % for FFA and 9.4 % for MAG.

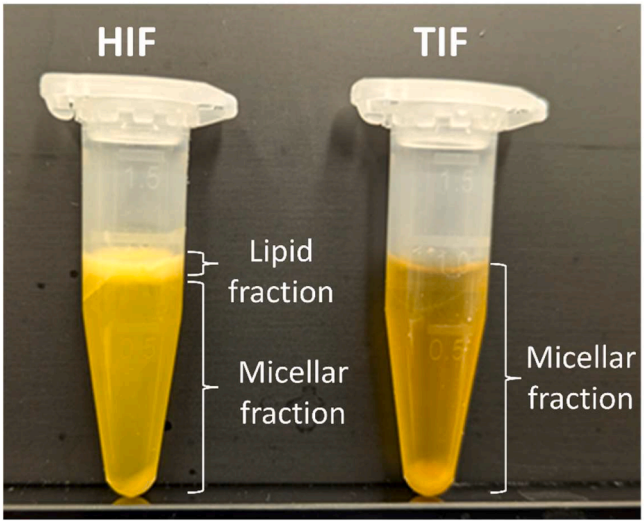

Fig. 4. Appearance of an early fed state HIF pool (left) and the TIF pool (right) after liquid meal administration following centrifugation (20 000 g, 37 °C, 30 min).

3.1.1.2. Bile salts. Fig. 6 compares the average bile salt composition of both HIF and TIF across the fasted and fed state pools. While taurochenodeoxycholic acid (TCDC) and glycochenodeoxycholic acid (GCDC) were present in both HIF and TIF, they were found in different

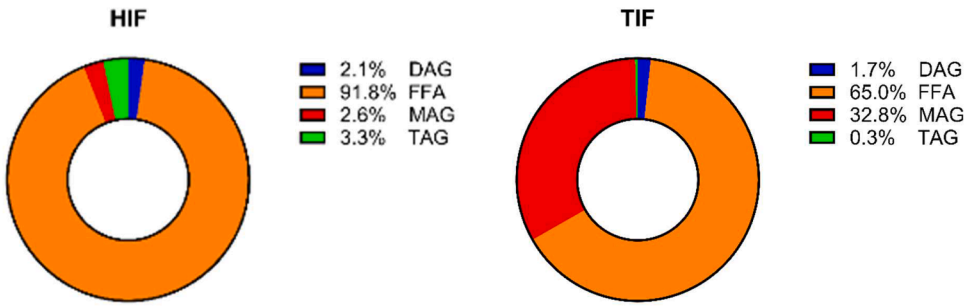

Fig. 5. Average composition of lipids and digestion products composition in early and late fed state HIF and TIF, after the administration of a liquid meal. TAG: triacylglycerides, DAG: diacylglycerides, MAG: monoacylglycerides, FFA: free fatty acids.

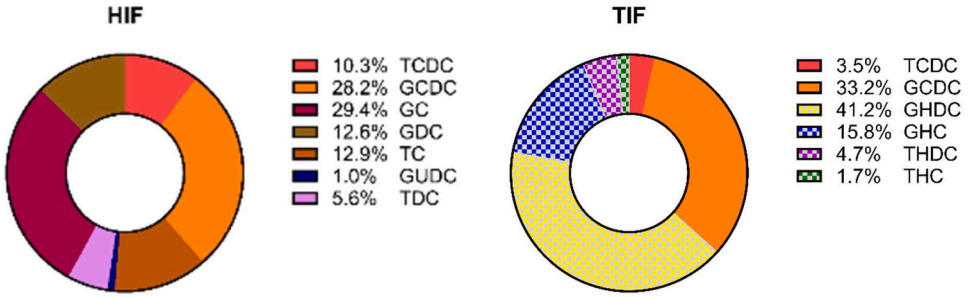

Fig. 6. Average bile salt composition of fasted and fed state HIF ($n = 21$) and TIF ($n = 3$), after the administration of a liquid meal. TCDC: taurochenodeoxycholic acid, GCDC: glycochenodeoxycholic acid, GC: glycocholic acid, GDC: glycodeoxycholic acid, TC: taurocholic acid, GUDC: glycoursodeoxycholic acid, TDC: taurodeoxycholic acid, GHDC: glycohyodeoxycholic acid, GHC: glycohyocholic acid, THDC: taurohyodeoxycholic acic and THC: taurohyocholic acid.

proportions. Moreover, a substantial portion of bile salts in TIF (62.8 %) consisted of derivates not found in humans, primarily based on the hyocholic acid backbone. Its structure differs from the cholic acid backbone, as it features an alcohol group at the R1 position instead of the R4 position (Holm et al., 2013). Our findings align with the bile salt composition of TIM-1 intestinal fluids reported by Pentafragka et al. (Pentafragka et al., 2022).

As illustrated in Fig. 3, a clear difference in total bile salt concentration was observed between HIF and TIF. In the fasted state, bile salt levels in TIF were elevated by a factor of 1.8 as compared to those in HIF. This discrepancy was even more pronounced in the total fed state samples, where the bile salt concentration in TIF was, on average, 5.3 times higher than in HIF, increasing from 9.3 mM in HIF to 49.5 mM in TIF.

Typically, bile salt concentrations do not differ considerably between the total and micellar samples. However, in the late fed state TIF, a notable reduction of 37.0 % was observed between the total and micellar fractions, even though a separate lipid fraction was not visible.

3.1.1.3. Phospholipids and total cholesterol. In the fasted state, phospholipids and total cholesterol in TIF were present in biorelevant concentrations. However, in both the early and late fed states, phospholipid and cholesterol levels were substantially higher in TIF as compared to HIF.

Additionally, similar to the pattern observed with bile salt concentrations in the late fed state, notable differences were found in TIF when the upper fraction was removed after centrifugation. Phospholipid concentrations were reduced by 15.7 %, and total cholesterol levels decreased by 57.6 % in the micellar fraction compared to the total sample. This finding was particularly interesting because, despite these reductions, no visible upper lipid fraction was observed after centrifugation. This suggests that bile salts, phospholipids, and cholesterol partition in a way that was not visually detectable.

3.1.1.4. pH and total protein. In both fasted and fed states, the pH in the tiny-TIM intestinal compartment was elevated by approximately 0.5 to 1 pH units as compared to the average pH value of the human duodenum. This higher pH value in tiny-TIM likely reflects the average in the human small intestine, rather than the pH value in more proximal regions. Additionally, no detectable proteins were present in fasted state TIF, while in the fed state, protein levels were slightly lower than those observed in HIF.

3.1.2. Solubilising capacity

Fig. 7 depicts the equilibrium solubility of seven lipophilic model drugs in both HIF and TIF across the fasted, early fed, and late fed states.

The most apparent observation in Fig. 7 is related to the comparison between total and micellar solubility. In HIF, the average solubilising capacity was much higher in the total sample (closed red dots) compared to the micellar fraction (open red dots): on average, a 13-fold difference was seen across all seven compounds. In TIF, however, only a marginal increase was observed from micellar solubility (open black dots) to total solubility (closed black dots), with an average fold increase of 1.2. This minimal change was in line with compositional data, which showed little difference in lipid concentration between the total and micellar samples in TIF.

Secondly, we evaluated the ability of TIF to predict the average solubility in HIF by calculating the TIF/HIF solubility ratios (Fig. 8). Two-fold differences (TIF/HIF = 0.5 and 2) are indicated with a dotted line and are considered to mark the acceptable range for comparison purposes. In the fasted state, the differences in solubility between TIF and HIF were relatively large for most compounds, with no consistent direction. Fold differences ranged from a 0.1-fold underprediction for itraconazole to a 3.3-fold overprediction for cabozantinib.

In the fed state, the micellar solubilizing capacity of TIF generally overpredicted that of HIF (Fig. 8, left graph), except for itraconazole, where an underprediction was observed. On average, TIF overestimated solubility in the micellar fraction of HIF by 3.3-fold.

For the total samples in the fed state (Fig. 8, right graph), solubilizing capacity predictions showed extensive variation, with no consistent

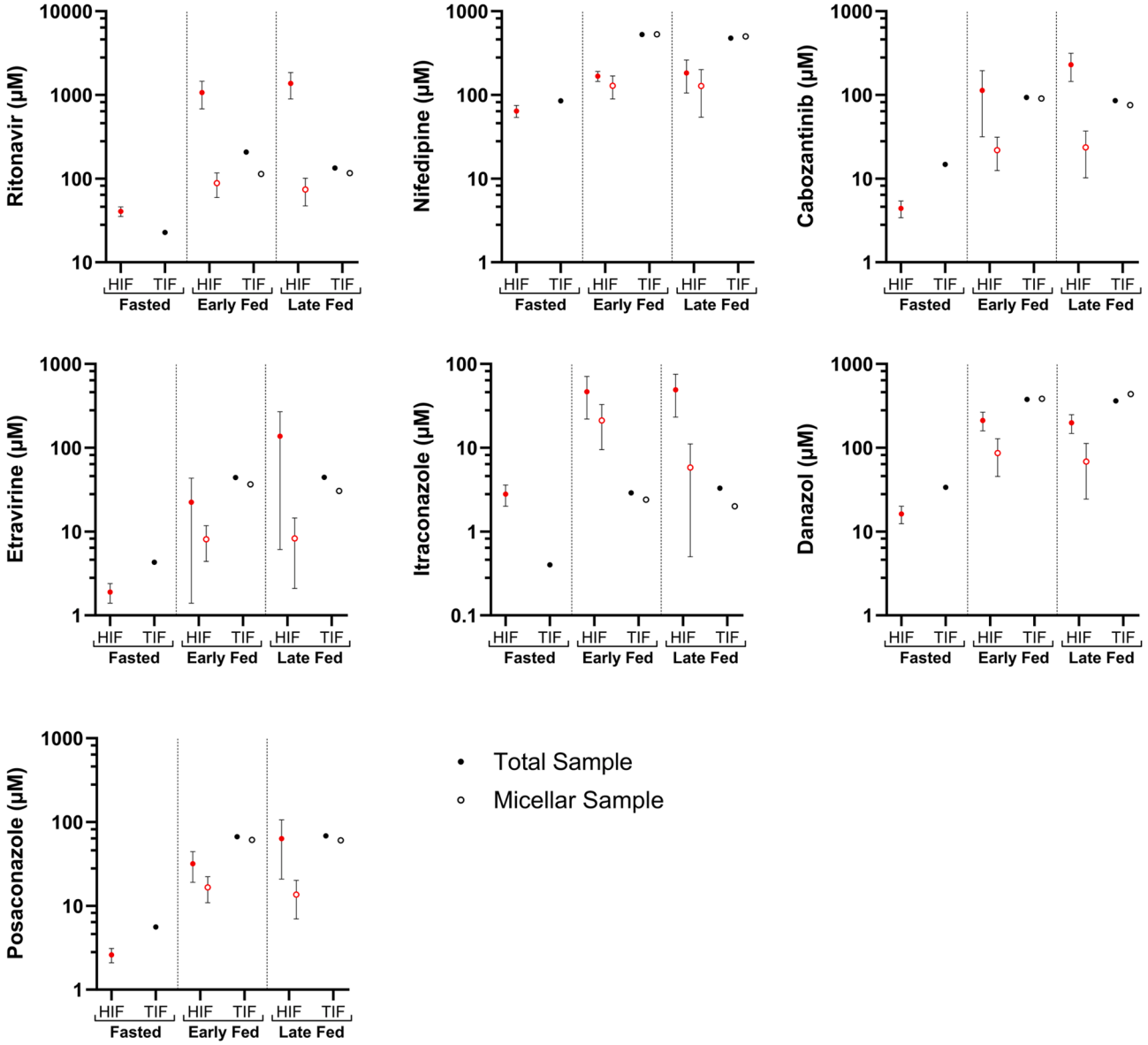

Fig. 7. Equilibrium solubility of the seven poorly water-soluble model drugs in HIF pools (red dots, mean ± SD, $n = 7$) and TIF (black dots, $n = 1$). Solubility was assessed in HIF and TIF representing the fasted state, early fed state and late fed state. In the fed state media, the total samples (closed dots) and micellar samples (open dots) were analysed separately.

direction, similar to the fasted state. For ritonavir and itraconazole, solubility was underpredicted in both the fasted and fed state fluids, while the solubility of cabozantinib, which was overpredicted in the fasted state, was now underpredicted. The solubilities of all other compounds were overpredicted by total fed state TIF.

Lastly, fed-to-fasted solubility ratios were calculated to compare TIF to HIF in providing a surrogate for food effect prediction. These ratios are shown in Fig. 9, based on solubility data in micellar samples (left graph) or total samples (right graph).

For micellar samples, the fed-to-fasted solubility ratios in TIF were consistently higher than those in HIF, leading to an overprediction of the ratio by an average of 2.0-fold (TIF/HIF). However, when total sample solubility values were used, the situation was reversed, with TIF underpredicting the fed-to-fasted solubility ratio by an average of 0.7-fold (TIF/HIF). This demonstrated a systematic discrepancy between the two systems depending on the sample type used for solubility assessment.

3.2. Composition and solubilising capacity of TIF after administration of a solid meal or a liquid meal

This section provides a detailed comparison of the composition and solubilizing capacity of TIF following the administration of either a liquid or a solid meal in both the early and late fed states.

Table 4 presents compositional parameters expressed as fold-differences, calculated by dividing the value obtained after a solid meal by that after a liquid meal. Overall, the composition of intestinal fluids did not differ much between the two meal types. Parameters least affected by meal type were bile salts and pH (fold difference between 0.88 and 1.27), both monitored by the system itself and not meal dependent. In contrast, parameters partially influenced by the meal, such as total lipids, phospholipids, and total cholesterol, exhibited greater differences. Total protein concentrations, however, remained relatively consistent across both meal conditions.

The limited compositional fluctuations between the solid meal and the liquid meal resulted in equally limited variations in solubilizing

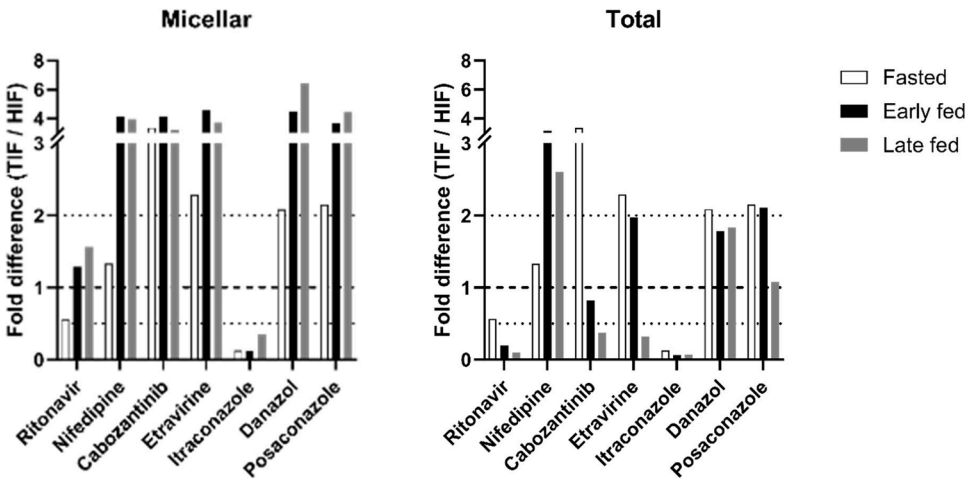

Fig. 8. Fold differences in solubilising capacity between TIF and HIF in the micellar samples (left) and the total samples (right). No difference (TIF/HIF = 1) is indicated with a bold dotted line. Two-fold differences (TIF/HIF = 0.5 and 2) are indicated with a dotted line.

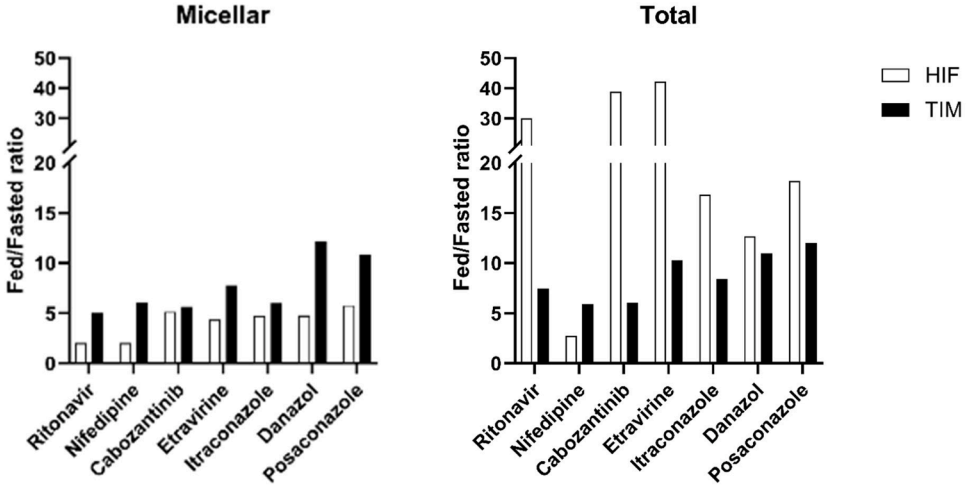

Fig. 9. Fed-to-fasted ratios using solubility data for seven model drugs in HIF (white bars) and TIF (black bars). Fed state solubility values were derived either from the micellar samples (left) or from the total sample (right).

Table 4
Fold-differences in TIF composition after the administration of either a solid meal or a liquid meal in the tiny-TIM model (solid meal/liquid meal).

Characteristic	Early fed state		Late fed state	
	Total sample	Micellar sample	Total sample	Micellar sample
Total lipids	1.29	1.08	1.38	1.47
Bile salts	1.03	0.88	1.00	1.27
Phospholipids	1.43	1.22	1.40	1.48
Total cholesterol	1.14	0.95	1.09	1.65
pH	1.01	/	1.01	/
Total protein	1.01	0.93	1.04	1.29

capacity. As shown in Table 5, fold differences in solubility were more pronounced for compounds highly influenced by the presence of lipid structures (total lipids, total cholesterol and phospholipids), such as ritonavir, cabozantinib and itraconazole.

4. Discussion

Unspecific food effects arise from multiple pathways, including postprandial variability in luminal conditions, absorption kinetics, drug distribution, metabolism, and elimination (Koziolek et al., 2019). Currently, multiple *in vitro* systems exist to explore the different pathways where food has an effect. Since the tiny-TIM is only intended to simulate luminal conditions, with no adequate permeation setup, one can only use it to predict the behaviour of a formulation in variable luminal conditions. To gain a more comprehensive understanding of food effects on oral bioavailability, it is necessary to integrate tiny-TIM data into *in silico* models that account for other physiological pathways as well.

Given the focus of tiny-TIM on simulating luminal conditions, our study aimed to evaluate its intestinal environment in terms of both composition and solubilizing capacity for lipophilic compounds, and to compare these results to corresponding data for human intestinal fluids (Goovaerts et al., 2024). The study design allowed for a detailed comparison, focusing on key aspects like phase separation, which has been observed in fed state HIF and results in distinct micellar and lipid fractions. By analysing both total samples and, after removal of the lipid fraction, micellar samples, we captured this important feature. Furthermore, we investigated the potential difference in the intestinal environment of tiny-TIM following the ingestion of both a solid meal and a liquid meal.

Table 5
Fold differences in equilibrium solubility of seven model compounds in TIF after the administration of either a solid meal or a liquid meal (solid meal/liquid meal ratio). Standard deviations (SD) were calculated using the propagation of error (PE)-method, using measurements performed in triplicate.

Compound	Early fed state				Late fed state			
	Total sample		Micellar sample		Total sample		Micellar sample	
	ratio	SD (PE)	ratio	SD (PE)	ratio	SD (PE)	ratio	SD (PE)
Ritonavir	1.15	0.02	1.28	0.45	0.79	0.39	0.86	0.19
Nifedipine	1.05	0.02	1.03	0.02	0.99	0.01	0.94	0.06
Cabozantinib	1.23	0.07	1.18	0.05	1.15	0.05	1.36	0.05
Etravirine	1.04	0.18	1.10	0.03	0.89	0.16	1.08	0.01
Itraconazole	1.26	0.17	1.15	0.07	1.14	0.22	1.61	0.29
Danazol	1.09	0.03	1.09	0.04	1.08	0.01	0.91	0.15
Posaconazole	1.06	0.03	1.02	0.06	0.93	0.01	0.97	0.03

4.1. Fasted state

Fasted state TIF was characterized by a low lipid concentration compared to fasted state HIF (TIF/HIF ratio of 0.27), and a relatively high bile salt concentration (TIF/HIF ratio of 1.8). Proteins were absent, and the pH was slightly elevated. This resulted in a monophasic fluid, with a solubilizing capacity that differed considerably from HIF. For only 2 out of 7 compounds, *i.e.*, ritonavir and nifedipine, the solubility differed less than twofold between TIF and HIF (Fig. 8). For the other compounds, the solubility was overpredicted in TIF. These results indicate that TIF is less predictive for the solubilizing capacity of fasted state HIF as compared to the commercially available fasted state simulated intestinal fluid (FaSSIF). In a previous study using the same compounds, we found a less than twofold difference in solubility between FaSSIF and HIF for 5 out of 7 compounds (Goovaerts et al., 2024). The tendency of TIF to overpredict the solubilizing capacity of HIF may be attributed to the elevated bile salt concentration and/or the different bile salt composition.

4.2. Fed state

4.2.1. TIF vs HIF

After ingestion of a liquid meal, fed state TIF was characterized by biorelevant lipid concentrations, though with a slower onset of gastrointestinal transfer compared to *in vivo* conditions, as evidenced by lower lipid concentrations in early fed state TIF. The most notable observation was the absence of visible phase separation in TIF (Fig. 4). Quantitatively, the lipid concentration in HIF decreased by 66 % following lipid fraction removal, compared to only a 20 % reduction in TIF after similar removal steps. The lack of a distinct lipid fraction in TIF implied that most lipids and digestion products were incorporated into the micellar phase. This shift in lipid distribution may be attributed to the significantly elevated bile salt concentration in TIF, which was 5.3 times higher than in HIF. The excess bile salts appeared to have solubilized all lipids into the micellar phase, resulting in a monophasic system (Hernell et al., 1990; Staggers et al., 1990). A directly proportional relationship between lipid presence in the micellar fraction and bile salt concentration was previously described by Goovaerts et al. (Goovaerts et al., 2024; Hernell et al., 1990; Staggers et al., 1990). Other factors that may have contributed to the altered physicochemical properties of the micellar phase in TIF include higher concentrations of phospholipids and cholesterol (likely due to their concomitant excretion with bile salts), and the presence of substantial levels of MAG in TIF (32.9 % (m/m)), which were virtually absent in HIF.

As highlighted in Section 3.1.2, the monophasic nature of TIF had a considerable impact on its solubilizing capacity. The micellar fraction of the tiny-TIM fluids, characterized by higher lipid and bile salt concentrations, exhibited a greater solubilizing capacity as compared to HIF, for all compounds except itraconazole. On average, a 3.3-fold increase in solubility (TIF/HIF) was observed across the studied compounds (see Fig. 8). Similar to the fasted state fluids, fed state TIF was less effective than commercially available fed state simulated intestinal fluid (FeSSIF) in predicting micellar HIF solubilizing capacity. The TIF/HIF solubility ratios indicated prediction errors larger than two-fold for all compounds except ritonavir. In contrast, the FeSSIF/HIF ratios were smaller than two-fold for all compounds except itraconazole (Goovaerts et al., 2024).

The total samples of TIF showed less consistent predictions, both in terms of the magnitude and direction, when compared to total HIF samples. Given that total TIF largely lacked a separate lipid fraction and exhibited similar solubility than its micellar fraction, the discrepancy between total TIF and HIF solubility largely depended on the additional solubilizing capacity provided by the lipid fraction in HIF. Consequently, drugs highly influenced by the lipid fraction in HIF, including ritonavir, cabozantinib and itraconazole, demonstrated the largest prediction errors.

4.2.2. Solid meal vs liquid meal

The shift from a liquid meal to a solid homogenised meal did not extensively affect the composition or solubilizing capacity of TIF. This limited variation could be attributed to the constant physiological parameters maintained during both runs, such as gastric emptying rates, intestinal pH and intestinal secretions. *In vivo*, however, different meal types may induce greater variability in luminal conditions, potentially resulting in further alterations in fluid composition and solubilizing capacity. To better understand this potential source of variability, further research involving *in vivo* aspiration studies after administration of solid meals is warranted.

4.3. Implications and future perspectives

The biorelevant simulation of exogenous factors such as total lipids and total protein in postprandial TIF, effectively mimicking the composition of total HIF samples, is a considerable achievement, considering the dynamic nature of the tiny-TIM system, which replicates key physiological processes like peristalsis, secretion, luminal transfer, and digestion. This makes the tiny-TIM system a valuable tool to predict *in vivo* drug release in fasted and fed state conditions, across a wide array of compounds (Liu et al., 2024). However, the overabundance of bile salts disrupts the balance of the system, significantly altering phase separation, resulting in an increased solubilizing capacity of the micellar fraction. This imbalance may be a key factor behind tiny-TIM's overprediction of food effects for certain low solubility compounds (Barker et al., 2014; Blanquet et al., 2004; Dickinson et al., 2012; Liu et al., 2024; López Mármol et al., 2022; Lloyd et al., 2020; Souliman et al., 2006, 2007; Verwei et al., 2016).

The elevated bile salt concentrations and their associated effects have not been detected in prior investigations. This raises important questions about the underlying reasons for this discrepancy. A previous study by Pentafragka *et al.* analyzed the larger TIM-1 system and found only a slight increase in bile salt concentrations (15–20 mM) compared to HIF, in contrast to the 40–50 mM observed in our study, suggesting this may be a tiny-TIM-specific characteristic (Pentafragka et al., 2022).

Another study by Verwei *et al.*, which compared both TIM-1 and tiny-TIM, did not assess bile salt concentrations but evaluated small-intestinal bioaccessibility profiles using low-solubility drugs, including an immediate-release suspension of posaconazole (Verwei et al., 2016). Consistent with our findings when comparing tiny-TIM to HIF, tiny-TIM presented a higher bioaccessible fraction in both the fasted and fed states than TIM-1, likely due to the higher solubilizing capacity of the fluids present in tiny-TIM. Since phase separation was not examined in that study, the discrepancy between the two systems may have been overlooked. However, we believe that accurately simulating aspects such as phase separation, is crucial for predicting the *in vivo* performance of oral formulations in fasted and fed state.

The key takeaway for future research is to reduce the bile salt concentration in tiny-TIM to more biorelevant levels, even if the bile salt composition differs. Short term, companies can further dilute the porcine bile to lower the rate of bile salt secretion into the intestinal compartment. A long-term solution should be found at the level of the manufacturer, where a change in the composition of the bile secretions, with reduced bile salt levels, can be implemented. Beyond this adjustment, our study also shed light on the role of surfactants and emphasized the importance of multi-phase simulated intestinal fluids in accurately predicting solubilizing capacity.

5. Conclusion

This study revealed that the conditions in the tiny-TIM intestinal compartment differed from those in the human intestinal environment in both fasted and fed state, primarily due to excessive bile salt concentrations in TIF. In the fed state, the excess bile salts likely solubilized all lipids into the micellar fraction, creating a single-phase fluid. Compared to HIF, TIF's micellar fraction was richer in bile salts, lipids, cholesterol, and phospholipids, significantly increasing its solubilizing capacity. As a result, the solubility of most of the lipophilic model compounds, except itraconazole, was overpredicted in the micellar fraction of TIF. To address this issue, we recommend reducing the bile salt concentrations in tiny-TIM to more biorelevant levels. This adjustment, combined with insights from our study on surfactants and multi-phase fluid simulation, could enhance the accuracy of tiny-TIM in predicting food effects. The findings of this work are critical to further enhance the predictive accuracy of *in vitro* models like tiny-TIM, ultimately contributing to more reliable drug product development and a better understanding of food effects on oral drug absorption.

Funding

This work was funded by AbbVie.

Declaration of Generative AI and AI-assisted technologies in the writing process

During the preparation of this work the authors used ChatGPT 4 in order to check spelling and grammar. After using this tool/service, the authors reviewed and edited the content as needed and take full responsibility for the content of the publication.

CRediT authorship contribution statement

Brecht Goovaerts: Writing – review & editing, Writing – original draft, Visualization, Methodology, Investigation, Formal analysis, Data curation, Conceptualization. **Álvaro López Mármol:** Writing – review & editing, Data curation, Conceptualization. **Joachim Brouwers:** Writing – review & editing, Supervision, Funding acquisition, Conceptualization. **Zahari Vinarov:** Writing – review & editing, Supervision. **Anura S. Indulkar:** Writing – review & editing, Funding acquisition. **Thomas B. Borchardt:** Writing – review & editing, Funding acquisition. **Patrick Augustijns:** Writing – review & editing, Supervision, Funding acquisition, Conceptualization. **Mirko Koziolek:** Writing – review & editing, Supervision, Resources, Funding acquisition, Conceptualization.

Declaration of competing interest

ALM, TBB and MK are employees of AbbVie and may own AbbVie stock. AI was an employee of AbbVie at the time the data presented in this work were generated. The authors declare that they have no competing financial interests or personal relationship that could have appeared to influence the work reported in this paper.

Acknowledgements

ZV gratefully acknowledges the support of the Bulgarian Ministry of Education and Science, under the National Research Program "VIHREN-2021", project 3D-GUT (№ KP-06-DV-3/15.12.2021).

Data availability

Data will be made available on request.

References

Barker, R., Abrahamsson, B., Kruusmägi, M., 2014. Application and validation of an advanced gastrointestinal *in vitro* model for the evaluation of drug product performance in pharmaceutical development. J. Pharm. Sci. 103 (11), 3704–3712. https://doi.org/10.1002/jps.24177.

Bennett-Lenane, H., O'Shea, J.P., O'Driscoll, C.M., Griffin, B.T., 2020. A retrospective biopharmaceutical analysis of >800 approved oral drug products: are drug properties of solid dispersions and lipid-based formulations distinctive? J. Pharm. Sci. 109 (11), 3248–3261. https://doi.org/10.1016/j.xphs.2020.08.008.

Bhardwaj, S.P., Arora, K.K., Kwong, E., Templeton, A., Clas, S.-D., Suryanarayanan, R., 2013. Correlation between molecular mobility and physical stability of amorphous itraconazole. Mol. Pharm. 10 (2), 694–700. https://doi.org/10.1021/mp300487u.

Blanquet, S., Zeijdner, E., Beyssac, E., Meunier, J.-P., Denis, S., Havenaar, R., Alric, M., 2004. A dynamic artificial gastrointestinal system for studying the behavior of orally administered drug dosage forms under various physiological conditions. Pharm. Res. 21 (4), 585–591. https://doi.org/10.1023/B:PHAM.0000022404.70478.4b.

Boyd, B.J., Bergström, C.A.S., Vinarov, Z., Kuentz, M., Brouwers, J., Augustijns, P., Brandl, M., Bernkop-Schnürch, A., Shrestha, N., Préat, V., Müllertz, A., Bauer-Brandl, A., Jannin, V., 2019. Successful oral delivery of poorly water-soluble drugs both depends on the intraluminal behavior of drugs and of appropriate advanced drug delivery systems. Eur. J. Pharmaceut. Sci. 137, 104967. https://doi.org/10.1016/j.ejps.2019.104967.

Butler, J., Hens, B., Vertzoni, M., Brouwers, J., Berben, P., Dressman, J., Andreas, C.J., Schaefer, K.J., Mann, J., McAllister, M., Jamei, M., Kostewicz, E., Kesisoglou, F., Langguth, P., Minekus, M., Müllertz, A., Schilderink, R., Koziolek, M., Jedamzik, P., Augustijns, P., 2019. *In vitro* models for the prediction of *in vivo* performance of oral dosage forms: recent progress from partnership through the IMI OrBiTo collaboration. Eur. J. Pharmaceut. Biopharmaceut. 136, 70–83. https://doi.org/10.1016/j.ejpb.2018.12.010.

Chiang, P.-C., Liu, J., Nagapudi, K., Wu, R., Dolton, M.J., Salehi, N., Amidon, G., 2022. Evaluating the IVIVC by combining tiny-tim outputs and compartmental PK model to predict oral exposure for different formulations of ibuprofen. J. Pharm. Sci. 111 (7), 2018–2029. https://doi.org/10.1016/j.xphs.2022.01.024.

Dickinson, P.A., Abu Rmaileh, R., Ashworth, L., Barker, R.A., Burke, W.M., Patterson, C. M., Stainforth, N., Yasin, M., 2012. An investigation into the utility of a multi-compartmental, dynamic, system of the upper gastrointestinal tract to support formulation development and establish bioequivalence of poorly soluble drugs. AAPS J. 14 (2), 196–205. https://doi.org/10.1208/s12248-012-9333-x.

FDA, 2002. Food-effect bioavailability and fed bioequivalence studies. J. Korean Pharmaceut. Sci. 34 (3), 223–228. https://doi.org/10.4333/KPS.2004.34.3.223.

Goovaerts, B., Brouwers, J., Vinarov, Z., Braeckmans, M., Indulkar, A.S., Lopez Marmol, A., Borchardt, T.B., Tack, J., Koziolek, M., Augustijns, P., 2024. Understanding the impact of lipids on the solubilizing capacity of human intestinal fluids. Mol. Pharm. https://doi.org/10.1021/acs.molpharmaceut.4c00944.

Hernell, O., Staggers, J.E., Carey, M.C., 1990. Physical-chemical behavior of dietary and biliary lipids during intestinal digestion and absorption. 2. Phase analysis and aggregation states of luminal lipids during duodenal fat digestion in healthy adult human beings. Biochemistry 29 (8), 2041–2056. https://doi.org/10.1021/bi00460a012.

Holm, R., Müllertz, A., Mu, H., 2013. Bile salts and their importance for drug absorption. Int. J. Pharm. 453 (1), 44–55. https://doi.org/10.1016/j.ijpharm.2013.04.003.

Infantes-Garcia, M.R., Verkempinck, S.H.E., Guevara-Zambrano, J.M., Hendrickx, M.E., Grauwet, T., 2021. Development and validation of a rapid method to quantify neutral lipids by NP-HPLC-charged aerosol detector. J. Food Compos. Anal. 102, 104022. https://doi.org/10.1016/j.jfca.2021.104022.

Koziolek, M., Alcaro, S., Augustijns, P., Basit, A.W., Grimm, M., Hens, B., Hoad, C.L., Jedamzik, P., Madla, C.M., Maliepaard, M., Marciani, L., Maruca, A., Parrott, N., Pávek, P., Porter, C.J.H., Reppas, C., van Riet-Nales, D., Rubbens, J., Statelova, M., Corsetti, M., 2019. The mechanisms of pharmacokinetic food-drug interactions—a perspective from the UNGAP group. Eur. J. Pharmaceut. Sci. 134, 31–59. https://doi.org/10.1016/j.ejps.2019.04.003.

Kumar, S., Jog, R., Shen, J., Zolnik, B., Sadrieh, N., Burgess, D.J., 2015. Formulation and performance of danazol nano-crystalline suspensions and spray dried powders. Pharm. Res. 32 (5), 1694–1703. https://doi.org/10.1007/s11095-014-1567-0.

Liu, J., Nagapudi, K., Chiang, P.-C., 2024. Evaluating utilization of tiny-TIM to assess the effect of food on the absorptions of oral drugs and its application on biopharmaceutical modeling. J. Pharm. Sci. https://doi.org/10.1016/j.xphs.2024.01.009.

Lloyd, R.S., Hingle, M.I., Bloomer, J.C., Charles, S.J., Butler, J.M., Paul, A., Zhu, X., Miller, B., D'Amico, D., Donald, A., Tal-Singer, R., Ambery, C., 2020. Negative food effect of danirixin: use of PBPK modelling to explore the effect of formulation and meal type on clinical PK. Pharm. Res. 37 (12), 233. https://doi.org/10.1007/s11095-020-02948-z.

López Mármol, Á., Fischer, P.L., Wahl, A., Schwöbel, D., Lenz, V., Sauer, K., Koziolek, M., 2022. Application of tiny-TIM as a mechanistic tool to investigate the *in vitro* performance of different itraconazole formulations under physiologically relevant conditions. Eur. J. Pharmaceut. Sci. 173, 106165. https://doi.org/10.1016/j.ejps.2022.106165.

Minekus, M., 2015. The TNO gastro-intestinal model (TIM). In: Verhoeckx, K., Cotter, P., López-Expósito, I., Kleiveland, C., Lea, T., Mackie, A., Requena, T., Swiatecka, D., Wichers, H. (Eds.), The Impact of Food Bioactives On Health: In vitro and Ex Vivo Models. Springer. http://www.ncbi.nlm.nih.gov/books/NBK500162/.

Pentafragka, C., Tomaszewska, I., Bellmann, S., Minekus, M., Schilderink, R., Vertzoni, M., McAllister, M., Reppas, C., 2022. *In vitro* simulation of the environment in the upper gastrointestinal lumen after drug administration in the fed state using the TIM-1 system and comparison with luminal data in adults. J. Pharm. Sci. 111 (1), 197–205. https://doi.org/10.1016/j.xphs.2021.10.010.

Schilderink, R., Protopappa, M., Fleth-James, J., Vertzoni, M., Schaefer, K., Havenaar, R., Kulla, I., Metzger, M., Reppas, C., 2020. On the usefulness of compendial setups and tiny-TIM system in evaluating the *in vivo* performance of oral drug products with various release profiles in the fasted state: case example sodium salt of A6197. Eur. J. Pharmaceut. Biopharmaceut. 149, 154–162. https://doi.org/10.1016/j.ejpb.2020.02.003.

Schöller-Gyüre, M., Kakuda, T.N., Raoof, A., De Smedt, G., Hoetelmans, R.M.W., 2009. Clinical pharmacokinetics and pharmacodynamics of etravirine. Clin. Pharmacokinet. 48 (9), 561–574. https://doi.org/10.2165/10895940-000000000-00000.

Souliman, S., Beyssac, E., Cardot, J.-M., Denis, S., Alric, M., 2007. Investigation of the biopharmaceutical behavior of theophylline hydrophilic matrix tablets using USP methods and an artificial digestive system. Drug Dev. Ind. Pharm. 33 (4), 475–483. https://doi.org/10.1080/03639040601128654.

Souliman, S., Blanquet, S., Beyssac, E., Cardot, J.-M., 2006. A level A in vitro/in vivo correlation in fasted and fed states using different methods: applied to solid immediate release oral dosage form. Eur. J. Pharmaceut. Sci. 27 (1), 72–79. https://doi.org/10.1016/j.ejps.2005.08.006.

Staggers, J.E., Hernell, O., Stafford, R.J., Carey, M.C., 1990. Physical-chemical behavior of dietary and biliary lipids during intestinal digestion and absorption. 1. Phase behavior and aggregation states of model lipid systems patterned after aqueous duodenal contents of healthy adult human beings. Biochemistry 29 (8), 2028–2040. https://doi.org/10.1021/bi00460a011.

Steuer, C., Huber, A.R., Bernasconi, L., 2016. Where clinical chemistry meets medicinal chemistry. Systematic analysis of physico-chemical properties predicts stability of common used drugs in gel separator serum tubes. Clin. Chim. Acta 462, 23–27. https://doi.org/10.1016/j.cca.2016.08.014.

van der Lee, R., Pfaffendorf, M., Koopmans, R.P., van Lieshout, J.J., van Montfrans, G.A., van Zwieten, P.A., 2001. Comparison of the time courses and potencies of the vasodilator effects of nifedipine and felodipine in the human forearm. Blood Press. 10 (4), 217–222. https://doi.org/10.1080/08037050152669738.

Vertzoni, M., Alsenz, J., Augustijns, P., Bauer-Brandl, A., Bergström, C., Brouwers, J., Müllerz, A., Perlovich, G., Saal, C., Sugano, K., Reppas, C., 2022. UNGAP best practice for improving solubility data quality of orally administered drugs. Eur. J. Pharmaceut. Sci. 168, 106043. https://doi.org/10.1016/j.ejps.2021.106043.

Verwei, M., Minekus, M., Zeijdner, E., Schilderink, R., Havenaar, R., 2016. Evaluation of two dynamic *in vitro* models simulating fasted and fed state conditions in the upper gastrointestinal tract (TIM-1 and tiny-TIM) for investigating the bioaccessibility of pharmaceutical compounds from oral dosage forms. Int. J. Pharm. 498 (1), 178–186. https://doi.org/10.1016/j.ijpharm.2015.11.048.

Vinarov, Z., Abrahamsson, B., Artursson, P., Batchelor, H., Berben, P., Bernkop-Schnürch, A., Butler, J., Ceulemans, J., Davies, N., Dupont, D., Flaten, G.E., Fotaki, N., Griffin, B.T., Jannin, V., Keemink, J., Kesisoglou, F., Koziolek, M., Kuentz, M., Mackie, A., Augustijns, P., 2021. Current challenges and future perspectives in oral absorption research: an opinion of the UNGAP network. Adv. Drug Deliv. Rev. 171, 289–331. https://doi.org/10.1016/j.addr.2021.02.001.

Williams, H.D., Ford, L., Han, S., Tangso, K.J., Lim, S., Shackleford, D.M., Vodak, D.T., Benameur, H., Pouton, C.W., Scammells, P.J., Porter, C.J.H, 2018. Enhancing the Oral Absorption of Kinase Inhibitors Using Lipophilic Salts and Lipid-Based Formulations. Mol. Pharm. 15 (12), 5678–5696. https://doi.org/10.1021/acs.molpharmaceut.8b00858.

Wiśniewski, J.R., Gaugaz, F.Z., 2015. Fast and sensitive total protein and peptide assays for proteomic analysis. Anal. Chem. 87 (8), 4110–4116. https://doi.org/10.1021/ac504689z.

Yu, J., Yu, D., Lane, S., McConnachie, L., Ho, R.J.Y., 2020. Controlled solvent removal from antiviral drugs and excipients in solution enables the formation of novel combination multi-drug-motifs in pharmaceutical powders composed of Lopinavir, Ritonavir and Tenofovir. J. Pharm. Sci. 109 (11), 3480–3489. https://doi.org/10.1016/j.xphs.2020.08.003.